Acta Crystallographica Section D
Biological Crystallography
ISSN 0907-4449

Improved crystals of *Thermus thermophilus* prolyl-tRNA synthetase complexed with cognate tRNA obtained by crystallization from precipitate

Anna Yaremchuk,[a,b]* Ivan Kriklivyi,[b] Stephen Cusack[a] and Mikhail Tukalo[a,b]

[a]European Molecular Biology Laboratory, Grenoble Outstation, c/o ILL, 156X, 38042 Grenoble, France, and [b]Instutute of Molecular Biology and Genetics, National Academy of Science of Ukraine, 252627 Kiev 143, Ukraine

Correspondence e-mail: yarem@embl-grenoble.fr

Received 16 September 1999
Accepted 29 November 1999

The complex between *Thermus thermophilus* prolyl-tRNA synthetase (ProRSTT) and its cognate tRNA has been crystallized using two different isoacceptors of $tRNA^{Pro}$. Similar bipyramidal crystals of the complexes of ProRSTT with the two different $tRNA^{Pro}$ isoacceptors grow within two weeks from 32% saturated ammonium sulfate solution. They belong to space group $P4_32_12$, with unit-cell parameters a = 143.1, b = 143.1, c = 228.6 Å. The crystals diffract weakly to a maximum resolution of 3.1 Å. Superior quality crystals were obtained by growing slowly from precipitate over 5–6 months. These are of the same space group but have slightly altered unit-cell parameters, a = 140.8, b = 140.8, c = 237.0 Å. These crystals diffract more strongly to at least 2.8 Å resolution and a complete data set to 2.85 Å resolution has been collected from a single crystal. Comparison of the packing in the two crystal forms shows that domain flexibility contributes to the presence of different crystal contacts in the two forms.

1. Introduction

On the basis of their sequence similarity and modular architecture, class II aminoacyl-tRNA synthetases can be partitioned into three subclasses (Cusack, 1995; Arnez & Moras, 1997). Subclass IIa synthetases (SerRS, ProRS, HisRS, GlyRS and ThrRS) have a homologous C-terminal putative anticodon-binding domain, with the exception of seryl-tRNA synthetase which does not contact the anticodon of its cognate tRNAs (Biou *et al.*, 1994; Cusack *et al.*, 1996*a*). In contrast, subclass IIb synthetases (LysRS, AspRS and AsnRS) have an N-terminal β-barrel anticodon-binding domain; structures showing the interactions of this domain with the anticodon stem-loop have been obtained for AspRS (Cavarelli *et al.*, 1993) and LysRS (Cusack *et al.*, 1996*b*). The mode of binding of tRNA to the class IIb anticodon-binding domain allows specific recognition of all three anticodon bases. Recently, the crystal structure of *T. thermophilus* prolyl-tRNA synthetase (ProRSTT) in complex with $tRNA^{Pro}$ has been determined at 3.5 Å resolution (Cusack *et al.*, 1998). Despite the modest resolution, this structure shows for the first time the mode of recognition of the class IIa anticodon-binding domain for the tRNA anticodon stem-loop. In contrast to the class IIb synthetases, the mode of binding of $tRNA^{Pro}$ to ProRSTT allows specific recognition of only two anticodon bases, G35 and G36, which are necessary and sufficient to identify all $tRNA^{Pro}$ isoacceptors. This is in agreement with biochemical experiments that have shown G35 and G36 to be important identity elements for recognition of $tRNA^{Pro}$ by prolyl-tRNA synthetase (Liu *et al.*, 1995; Stehlin *et al.*, 1998).

Here, we report the crystallization and preliminary crystallographic studies of two crystal forms of the complex of ProRSTT with two isoacceptors of $tRNA^{Pro}$. The second crystal form has similar but distinct unit-cell parameters to the first, shows much improved diffraction quality and is obtained by a special crystallization procedure from precipitate. This crystal form has been used for new data collections to 2.85 Å resolution. Crystallization of substrate-free ProRSTT is reported in the accompanying paper (Yaremchuk *et al.*, 2000).

2. Results and discussion

A search for crystallization conditions was undertaken using ProRSTT with two different $tRNA^{Pro}$ isoacceptors and using the hanging-drop vapour-diffusion method. For some of these experiments, a non-hydrolyzable prolyl-adenylate analogue {5′-*O*-[*N*-(prolyl)-sulfamoyl]adenosine} was used for co-crystallization or soaking (Ueda *et al.*, 1991). The synthesis of this compound and its interactions with ProRSTT will be described elsewhere (S. Cusack, A. Yaremchuk, M. Grøtli & M. Tukalo, unpublished results).

The same tetragonal crystal form, denoted form 1, of the complex of ProRSTT with either wild-type *T. thermophilus* $tRNA_1^{Pro}$(GGG) or $tRNA_2^{Pro}$(CGG) was obtained at 293 K from 10 µl drops containing 12% saturated ammo-

nium sulfate, 50 m*M* Tris–maleate (pH 7.5), 5 m*M* $MgCl_2$, 2 m*M* DTT, 2 m*M* NaN_3 with ProRSTT at 4 mg ml^{-1} and $tRNA_1^{Pro}$ or $tRNA_2^{Pro}$ at 1.85 mg ml^{-1}, corresponding to a molar ratio of enzyme:tRNA of 1:2, equilibrated with 32% saturated ammonium sulfate in 50 m*M* Tris–maleate pH 7.5. Octahedral crystals grew to a maximum size of 400 × 400 × 400 µm within one week and belong to space group $P4_32_12$ (No. 96), with unit-cell parameters a = 142.7, b = 142.7, c = 230.9 Å for $tRNA_1^{Pro}$(GGG) and a = 143.1, b = 143.1, c = 228.6 Å for $tRNA_2^{Pro}$(CGG). The crystals diffract to a maximum resolution of 3.1 Å, but the weak higher resolution diffraction disappears within a few images owing to radiation damage, even when the crystals are frozen to 100 K using glycerol as a cryo-protectant. The crystal quality and the limited availability of large crystals only permitted data sets to be collected to 3.6 Å resolution with $tRNA_1^{Pro}$ and to 3.5 Å resolution with $tRNA_2^{Pro}$, using two crystals in each case. The ProRSTT–tRNA complex structure was solved by molecular replacement using the 2.43 Å refined model of the ProRSTT dimer (S. Cusack, A. Yaremchuk & M. Tukalo, unpublished results) as a search model. The crystal structure of the ProRSTT–$tRNA^{Pro}$ complex is described elsewhere (Cusack *et al.*, 1998).

A second tetragonal crystal form, denoted form 2, similar to that described above but diffracting to 2.8 Å resolution, has been obtained by the method of crystallization from precipitate. Drops of the same composition as described above were equilibrated with 55% saturated ammonium sulfate in 50 m*M* Tris–maleate (pH 7.5) for 1–2 d at 279 K. Under these conditions, the macromolecules rapidly form an amorphous precipitate. Subsequently, the drops were transferred to 293 K followed by a step-by-step decrease of the ammonium sulfate concentration in the reservoir to 40% saturation over a period of 1–2 months. Usually, a few microcrystals were visible after 1–2 months. They grow slowly over a 5–6 month period to a maximum size of 360 × 360 × 360 µm at the expense of the precipitate. We have no evidence that the crystal growth is by a mechanism of Ostwald ripening, *i.e.* larger crystals growing at the expense of smaller ones (Ng *et al.*, 1996).

Crystals grown in this fashion belong to the same space group as previously found ($P4_32_12$) but with slightly altered unit-cell parameters, a = 140.8, b = 140.8, c = 237.0 Å. The a and b axes decrease by about 2 Å, whereas the c-axis dimension is systematically increased by about 6–8 Å (Table 1). These crystals diffract more strongly to higher resolution (at least to 2.8 Å) and with less diffuse scattering than the previous crystal form; they are also more stable to radiation damage when frozen to 100 K. Complete data sets have been obtained at 3.0 Å resolution on the ProRSTT–$tRNA^{Pro}$(CGG) binary complex crystal and at 2.85 Å resolution on a ternary complex after soaking a crystal with a sulphamoyl analogue of prolyl-adenylate (Table 1). These structures and the observed substrate-induced conformational changes in ProRSTT will be described elsewhere (S. Cusack, A. Yaremchuk & M. Tukalo, unpublished results).

The structure of the complex from form 2 crystals has been refined to an R factor and R_{free} of 0.21 and 0.24, respectively, at 2.85 Å resolution (S. Cusack, A. Yaremchuk & M. Tukalo, submitted). The asymmetric unit comprises one ProRSTT dimer (with subunits A and B) and one tRNA molecule. This was used to obtain a model for the form 1 crystals by molecular replacement followed by rigid-body refinement, firstly of the complex and secondly with the two ProRSTT subunits and the tRNA treated separately (R_{free} decreases from 0.371 to 0.336), using *CNS* (Brunger *et al.*, 1998). Inspection of maps shows clearly that the ProRSTT dimer is essentially the same in both crystal forms, apart from a small rotation of the anticodon domain of subunit A to which no tRNA is bound (Fig. 1*a*). Slight flexibility of this domain is also observed in the four independent copies of the ProRSTT subunit in crystals of the uncomplexed enzyme (S. Cusack, A. Yaremchuk & M. Tukalo, unpublished results). Further rigid-body refinement, in which this domain (residues 286–379) was allowed to move, led to a final model for form 2 with an R factor and R_{free} of 0.321 and 0.309, respectively, for all data in the resolution range 20–3.5 Å,

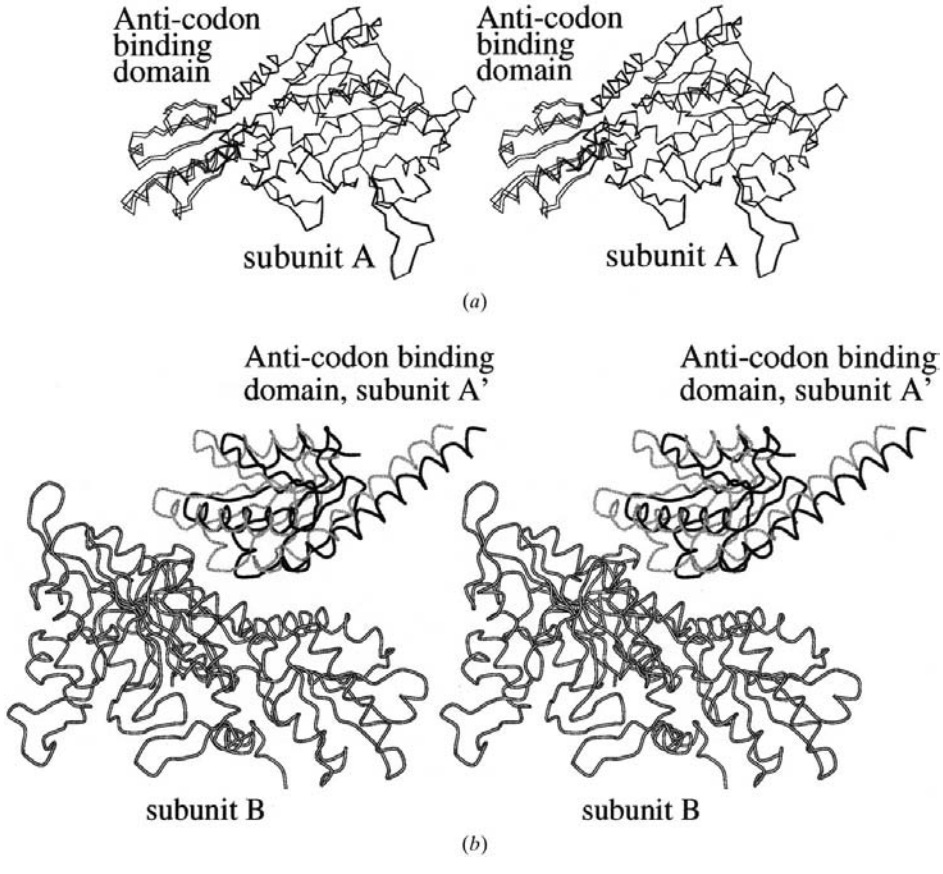

Figure 1
(*a*) Superposition of the C^{α} trace of subunit A of the prolyl-tRNA synthetase dimer in form 1 and form 2 crystals showing the slight rotation of the anticodon-binding domain. (*b*) Crystal contact between subunit B of the ProRSTT dimer and the anticodon-binding domain of a crystal symmetry-related subunit A (denoted A'). A' is related to A by the crystal symmetry $-y, -x, \frac{1}{2} - z$ in space group 96. This figure was obtained after superposition of subunit B from the two crystal forms. The anticodon-binding domain from subunit A' is grey for form 1 and black for form 2. In both crystal forms, the crystal contact involves the same regions but the residue interactions are different in detail (see text).

Table 1
Data-collection statistics for two crystal forms of the ProRSTT–tRNA^{Pro}(CGG) complex.

Crystal form	Original, form 1	New, form 2
Nature of complex	Binary complex ProRSTT–tRNA^{Pro}(CGG)	Ternary complex ProRSTT–tRNA^{Pro}(CGG) soaked with prolyl-adenylate analogue
Beamline	ID2 (ESRF)	ID2 (ESRF)
Detector	300 mm MAR IP	345 mm MAR IP
Wavelength (Å)	0.99	0.99
Detector distance (mm)	450	470
Exposure per image (s degree^{-1})	60	20
Space group	$P4_32_12$	$P4_32_12$
Unit-cell dimensions (Å)	$a = b = 143.1$, $c = 228.6$	$a = b = 140.8$, $c = 237.0$
Volume (Å^3)	4681181.6	4698439.7
No. of crystals	2	1
Resolution (Å)	20–3.5†	20–2.85
Total reflections	69329†	221758
Unique reflections	27011†	55013
Average redundancy‡	2.6 (2.1)†	4.0 (2.8)
Completeness‡	89.1 (73.1)§	98.2 (96.1)
R_{merge}‡	0.098 (0.263)†	0.084 (0.298)

† These values differ slightly from Table 1 of Cusack *et al.* (1998) owing to rescaling of the data to include low-resolution data to 20 Å. ‡ The values in brackets are for the highest resolution shell. § The completeness given here corrects that erroneously given in Table 1 of Cusack *et al.* (1998).

including anisotropic *B*-factor and solvent correction.

Comparison of the crystal packing in the two crystal forms shows that the rotation of the anticodon domain of subunit *A*, coupled with the unit-cell variation, leads to a significant change in the crystal contact involving this domain and subunit *B* from a crystal symmetry-related molecule (Fig. 1*b*). Although the same regions are involved in the contact, the actual residue interactions are quite different owing to a significant relative movement of the contacting molecules. For instance, in form 2 the hydroxyl group of Tyr393*B* makes a hydrogen bond (distance 2.8 Å) with the carbonyl O atom of Glu356*A*, whereas in form 1 these two atoms are too far apart to interact (about 7 Å). Note that the limited resolution of the form 1 crystals does not permit a detailed description of the side-chain interactions. Several examples have been reported in the literature of improved diffraction quality occurring within the same crystal *via* crystal dehydration and shrinkage of unit-cell dimensions, *e.g.* HIV-RT (Stammers *et al.*, 1994), EfTu-Ts (Schick & Jurnak, 1994; Kawashima *et al.*, 1996), NF-κB p52 (Cramer & Muller, 1997). In the case of the ProRSTT–tRNA^{Pro} complex, although the beneficial effect on diffraction quality is the same, the mechanism seems to be different. Firstly, between the two crystal forms, the unit-cell volume hardly varies, owing to changes in the $a = b$ axes and the c axis of opposite sign (Table 1). Secondly, an experiment in which a crystal of the first form was soaked at higher ammonium sulfate concentration (38% saturation) before measurement did not demonstrate transformation from form 1 to form 2, although this possibility cannot be ruled out. Furthermore, as discussed above, the crystal packing changes subtly but significantly. Although these observations do not directly explain why one crystal form diffracts much better the other, nor why the method of growth should lead to this difference, we suggest that, unlike the cases of dehydration and shrinkage cited above, in the case of the ProRSTT–tRNA^{Pro} complex two very similar but essentially different, in the sense of non inter-transformable, crystal forms exist. Domain flexibility combined with altered intermolecular side-chain interactions perhaps resulting from the different initial ammonium sulfate concentrations seem to be responsible for this phenomenon.

The authors thank members of the EMBL/ESRF Joint Structural Biology Group (JSBG), especially Jonathan Grimes and Bjarne Rasmussen, for support in the measurements on beamline ID2 at the ESRF. The research of MT was supported in part by an International Research Scholar's award from the Howard Hughes Medical Institute.

References

Arnez, J. G. & Moras, D. (1997). *Trends Biochem. Sci.* **22**, 211–216.
Biou, V., Yaremchuk, A., Tukalo, M. & Cusack, S. (1994). *Science*, **263**, 1404–1410.
Brunger, A. T., Adams, P. D., Marius Clore, G., DeLano, W. L., Gros, P., Grosse-Kunstleve, R. W., Jiang, J.-S., Kuszewski, J., Nilges, M., Pannu, N. S., Read, R. J., Rice, L. M., Simonson, T. & Warren, G. L (1998). *Acta Cryst.* D**54**, 905–921.
Cavarelli, J., Rees, B., Ruff, M., Thiery, J.-C. & Moras, D. (1993). *Nature (London)*, **362**, 181–184.
Cramer, P. & Muller, C. (1997). *FEBS Lett.* **405**, 373–377.
Cusack, S. (1995). *Nature Struct. Biol.* **2**, 824–831.
Cusack, S., Yaremchuk, A., Kriklivyi, I. & Tukalo, M. (1998). *Structure*, **6**, 101–108.
Cusack, S., Yaremchuk, A. & Tukalo, M. (1996*a*). *EMBO J.* **15**, 2834–2842.
Cusack, S., Yaremchuk, A. & Tukalo, M. (1996*b*). *EMBO J.* **15**, 6321–6334.
Kawashima, T., Berthet-Colominas, C., Cusack, S. & Leberman, R. (1996). *Acta Cryst.* D**52**, 799–805.
Liu, H., Peterson, R., Kessler, J. & Musier-Forsyth, K. (1995). *Nucleic Acids Res.* **23**, 1665–1669.
Ng, J. D., Lorber, B., Witz, J., Théobald-Dietrich, A., Kern, D. & Giegé, R. (1996). *J. Cryst. Growth*, **168**, 50–62.
Schick, B. & Jurnak, F. (1994). *Acta Cryst.* D**50**, 563–568.
Stammers, D. K., Somers, D. O'N., Ross, C. K., Kirby, I., Ray, P. H., Wilson, J. E., Norman, M., Ren, J. S., Esnouf, R. M., Garman, E. F., Jones, E. Y. & Stuart, D. I. (1994). *J. Mol. Biol.* **242**, 586–588.
Stehlin, C., Burke, B., Yang, F., Liu, H., Shiba, K. & Musier-Forsyth, K. (1998). *Biochemistry*, **37**, 8605–8623.
Ueda, H., Shoku, Y., Hayashi, N., Mitsunaga, J., In, Y., Doi, M., Inoue, M. & Ishida, T. (1991). *Biochem. Biophys. Acta*, **1080**, 126.
Yaremchuk, A., Cusack, S. & Tukalo, M. (2000). *Acta Cryst.* D**56**, 195–196.